Stochastic Lindemann Kinetics for Unimolecular Gas-Phase Reactions

ARTICLE *in* THE JOURNAL OF PHYSICAL CHEMISTRY A · JULY 2013

Impact Factor: 2.69 · DOI: 10.1021/jp402675s · Source: PubMed

2 AUTHORS, INCLUDING:

Arti Dua

Indian Institute of Technology Madras

28 PUBLICATIONS **177** CITATIONS

SEE PROFILE

THE JOURNAL OF PHYSICAL CHEMISTRY A

Article

pubs.acs.org/JPCA

Stochastic Lindemann Kinetics for Unimolecular Gas-Phase Reactions

Soma Saha and Arti Dua*

Department of Chemistry, Indian Institute of Technology, Madras, Chennai-600036, India

ABSTRACT: Lindemann, almost a century ago, proposed a schematic mechanism for unimolecular gas-phase reactions. Here, we present a new semiempirical method to calculate the effective rate constant in unimolecular gas-phase kinetics through a stochastic reformulation of Lindemann kinetics. Considering the rate constants for excitation and de-excitation steps in the Lindemann mechanism as temperature dependent empirical parameters, we construct and solve a chemical master equation for unimolecular gas-phase kinetics. The effective rate constant thus obtained shows excellent agreement with experimental data in the entire concentration range in which it is reported. The extrapolated values of the effective rate constant for very low and very high concentrations of inert gas molecules are in close agreement with values obtained using the Troe semiempirical method. Stochastic Lindemann kinetics, thus, provides a simple method to construct the full falloff curves and can be used as an alternative to the Troe semiempirical method of kinetic data analysis for unimolecular gas-phase reactions.

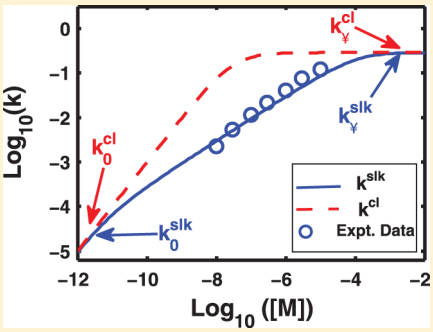

INTRODUCTION

Unimolecular reactions such as dissociation and isomerization reactions in the gas phase appear to be first-order in the reactants. However, at low pressures, such reactions show second-order kinetics. In 1922, F. Lindemann proposed a mechanism to explain this rather puzzling behavior by splitting the unimolecular reaction into elementary steps represented by[1]

$$A + M \underset{k_{-1}}{\overset{k_1}{\rightleftharpoons}} A^* + M \overset{k_2}{\rightarrow} P$$

According to the Lindemann mechanism, when a gas molecule A undergoes a bimolecular collision with an inert gas molecule M with rate constant k_1, the molecule A is raised to its higher vibrational level resulting in an excited molecule A^*. Once in the higher vibrational state, the excited molecule A^* can either lose its extra energy in another bimolecular collision with rate constant k_{-1} or form a product with rate constant k_2. In the steady-state condition, when the de-excitation of the excited molecules happens faster than the excitation, the rate of product formation is given by $(d[P]/dt) = k^{cl}[A]$, yielding the classical Lindemann equation,

$$k^{cl} = \frac{k_m k_2}{(k_{-m} + k_2)} \quad (1)$$

where k^{cl} is the classical effective rate constant, $k_m = k_1[M]$ and $k_{-m} = k_{-1}[M]$ are the pseudo first-order rate constants. The limiting values of the effective rate constant at low and high concentrations of inert gas molecules are $k_0^{cl} = k_1[M]_0$ and $k_\infty^{cl} = k_1k_2/k_{-1}$, respectively.

Chemical reactions are intrinsically stochastic and depends on random collisional events for excitation and de-excitation of molecules. The classical Lindemann equation based on the deterministic mass action kinetics cannot account for such effects and, therefore, does not compare well with experiments. Theoretical techniques based on the master equation (ME) approach include the random effects of collisional excitation/de-excitation and unimolecular decomposition in the master equation. The master equation, written for the time evolution of the probability density $P(E,t)$ that a molecule at time t has energy E, mainly depends on the transition probability density of going from one energy state to another upon collision and energy-dependent effective rate constant for decomposition $k(E)$. The latter is calculated from the inverse Laplace transform of the high pressure effective rate constant, $k_\infty(T)$. However, in most cases the master equation can only be solved numerically making it a relatively complex and computationally expensive method for data analysis.

The kinetic data for unimolecular gas-phase reactions are often analyzed using well-known theoretical methods like the RRKM[2−5] and ME[6−8] approaches. However, in spite of the predictive nature of the latter, it is the simplicity of the Troe semiempirical (TSE) method,[9−21] which makes it the most widely used technique for data analysis among kineticists. The TSE method considers the effective rate constant at low (k_0) and high (k_∞) concentrations of inert gas molecules as empirical input parameters. It interpolates k_0 and k_∞ to the intermediate concentration regime, and works well when the experimental data are available near these asymptotic concentrations of the inert gas molecules. In most kinetic studies, however, the low and high concentration regimes remain experimentally inaccessible, making the empirical estimates for k_0 and k_∞ unreliable. Thus, the TSE is often used in conjunction with the RRKM/ME theory to obtain the empirical input parameters. Thus, it remains desirable to have a complementary theoretical approach that, instead of interpolating from inaccessible asymptotic data points, extrapolates from the experimentally accessible regions to

Received: March 18, 2013
Revised: July 23, 2013
Published: July 23, 2013

construct the full falloff curves. We present such an approach below by reformulating Lindemann kinetics stochastically.

Here, we reformulate Lindemann kinetics to account for the intrinsic stochasticity of chemical reactions. We consider the rate of excitation and de-excitation steps in the Lindemann mechanism as the empirical parameters and construct a chemical master equation description for the reaction kinetics. In this stochastic Lindemann kinetics (SLK), the joint probability distribution of the discrete number of reactants, intermediates, and products at time t is the fundamental object whose dynamics is prescribed by the chemical master equation (CME). In a small interval of time, the number of molecules of each type, as a result of random collisions, can either change by unity or remain the same. These changes are specified through the CME transition probabilities, for each step in the Lindemann mechanism. The SLK thus describes a multivariate stochastic process, which we solve exactly to obtain an expression for the waiting time distribution for the formation of first product. The first moment of this probability distribution yields the mean waiting time. The reciprocal of the mean time of waiting is related to the effective rate constant, which is compared with the experimental data for the decomposition of N_2O_5,[22] iso-C_3H_7,[23] isobutane,[24] n-butane,[24] isomerization of cyclopropane,[25] methyl isocyanide,[26] and 3-methyl cyclobutene,[27] at different temperatures. The SLK approach shows excellent agreement with the experimental data in the entire concentration range of inert gas molecules in which the experimental data are accessible. Most importantly, it provides accurate estimates for the effective rate constant over the range where the experimental data are inaccessible, in complete agreement with the more involved RRKM theory.

STOCHASTIC LINDEMANN KINETICS

In a stochastic approach, corresponding to each reactant, product, and intermediate, there is a discrete random variable which has a finite number of positive integral states, as allowed by the stoichiometry. The state is specified by the number of molecules of each type in the system. If n_a, n_{a^*}, and n_p represent the number of A, A^*, and P, respectively, at time t and $N = n_a + n_{a^*} + n_p$ is the number of A molecules at any time $t = 0$, then the multivariate CME for the time-evolution of the joint probability distribution $P(n_a,n_{a^*},n_p,t)$, based on Lindemann mechanism, can be written as

$$\begin{aligned}\frac{\partial P(n_a, n_{a*}, n_p, t)}{\partial t} &= k_m(n_a + 1)P(n_a + 1, n_{a*} - 1, n_p, t)\\ &+ k_{-m}(n_{a*} + 1)P(n_a - 1, n_{a*} + 1, n_p, t)\\ &+ k_2(n_{a*} + 1)P(n_a, n_{a*} + 1, n_p - 1, t)\\ &- [k_m n_a + (k_{-m} + k_2)n_{a*}]P(n_a, n_{a*}, n_p, t)\end{aligned} \tag{2}$$

A distinct feature of the SLK approach is that it includes the effects of random collisions in the "rate equation" rendering the rate constants, k_1, k_{-1}, and k_2 as temperature dependent empirical parameters. The analytical solution of the CME, eq 2, has to satisfy the constraint $n_a + n_{a^*} + n_p = N$, resulting in the probability distribution $P(N-n_{a^*}-n_p,n_{a^*},n_p,t|N)$, which we abbreviate as $P(n_{a^*},n_p,t|N)$.

For a univariate stochastic process, stochastic trajectories can be described by either using the counting process description, which counts the number of products formed in a given time t or using the point process description, which specifies the waiting time, τ, for the formation of first product.[28,29] In a recent work,[30] we have used the connection between the counting and point processes[31] to describe the turnover statistics of a multivariate stochastic process to show that the waiting time distribution for the formation of first product is given by

$$w(\tau|N) = -\sum_{n_{a*}} \frac{\partial P(n_{a*}, 0, t|N)}{\partial t}\bigg|_{t=\tau} \tag{3}$$

where τ is the waiting time for the formation of first product. Using the generating function method, eq 2 can be solved to obtain the exact expression for the waiting time distribution for the formation of first product. The Appendix provides the details of the calculation. The result is an *exact* expression for the waiting time distribution, given by

$$\begin{aligned}w(\tau|N) &= \frac{Nk_2k_m}{(2\lambda_1)^N}[e^{-(\lambda_2-\lambda_1)\tau} - e^{-(\lambda_2+\lambda_1)\tau}]\\ &\times [(\lambda_1 + \lambda_2)e^{-(\lambda_2-\lambda_1)\tau} + (\lambda_1 - \lambda_2)e^{-(\lambda_2+\lambda_1)\tau}]^{N-1}\end{aligned} \tag{4}$$

where $\lambda_1 = ((k_m + k_{-m} + k_2)^2 - (4k_mk_2/2))^{1/2}$ and $\lambda_2 = (k_m + k_{-m} + k_2)/2$. The equation for the waiting time distribution for the formation of first product is the key result of the present work. From the first moment of the distribution we can obtain the mean waiting time and the effective rate constant.

Mean Waiting Time and Effective Rate Constant. The first moment of the waiting time distribution yields the mean waiting time for the formation of first product, $\langle\tau\rangle = \int_0^\infty \tau w(\tau|N)d\tau$. For a single molecule, $N = 1$, the waiting time for the formation of product is given by $\langle\tau\rangle = ((k_{-m} + k_2)/(k_mk_2))$, which shows that $k^{slk} = \langle\tau\rangle^{-1}$.

There is no closed form analytical expression for the mean waiting time for $N \gg 1$. However, an approximate analytical expression for the mean waiting time at large N can be obtained in the limit of $k_{-m} + k_2 \gg k_m$, which amounts to the steady-state approximation in the deterministic kinetics, resulting in

$$\begin{aligned}w(\tau|N) &= N\Delta e^{-N\Delta\tau}[1 - e^{-(2\lambda_2-\Delta)\tau}]\\ &\times\left[1 - \frac{\Delta(N-1)}{2\lambda_2}e^{-(2\lambda_2-\Delta)\tau}\right]\end{aligned} \tag{5}$$

where $\lambda_1-\lambda_2 \approx -\Delta$, $\lambda_1 + \lambda_2 \approx 2\lambda_2$ and $\Delta = k_mk_2/(k_{-m}+k_2)$. From the above equation, the mean waiting time for the formation of first product, $\langle\tau\rangle$ is given by

$$\begin{aligned}\langle\tau\rangle = \frac{1}{N\Delta}\Bigg[1 &- \frac{(N-1)N^2\Delta^6}{k_mk_2(k_mk_2 + (N-1)\Delta^2)^2}\\ &- \frac{N^2\Delta^4}{(k_mk_2 + (N-1)\Delta^2)^2}\\ &+ \frac{(N-1)N^2\Delta^6}{k_mk_2(2k_mk_2 + (N-2)\Delta^2)^2}\Bigg]\end{aligned} \tag{6}$$

In the limit of infinitely large and vanishingly small concentration of inert gas molecules M, only the zeroth order contribution in the above expression survives, yielding

$$\frac{\langle\tau\rangle^{-1}}{N} = \Delta = \frac{k_2k_m}{k_{-m} + k_2} \tag{7}$$

which recovers the classical Lindemann equation if the initial rate of product formation $v = k^{cl}[A]_0$ is interpreted as the reciprocal of mean waiting time for the formation of first product $\langle\tau\rangle^{-1}$, as was

dx.doi.org/10.1021/jp402675s | J. Phys. Chem. A 2013, 117, 7661−7669

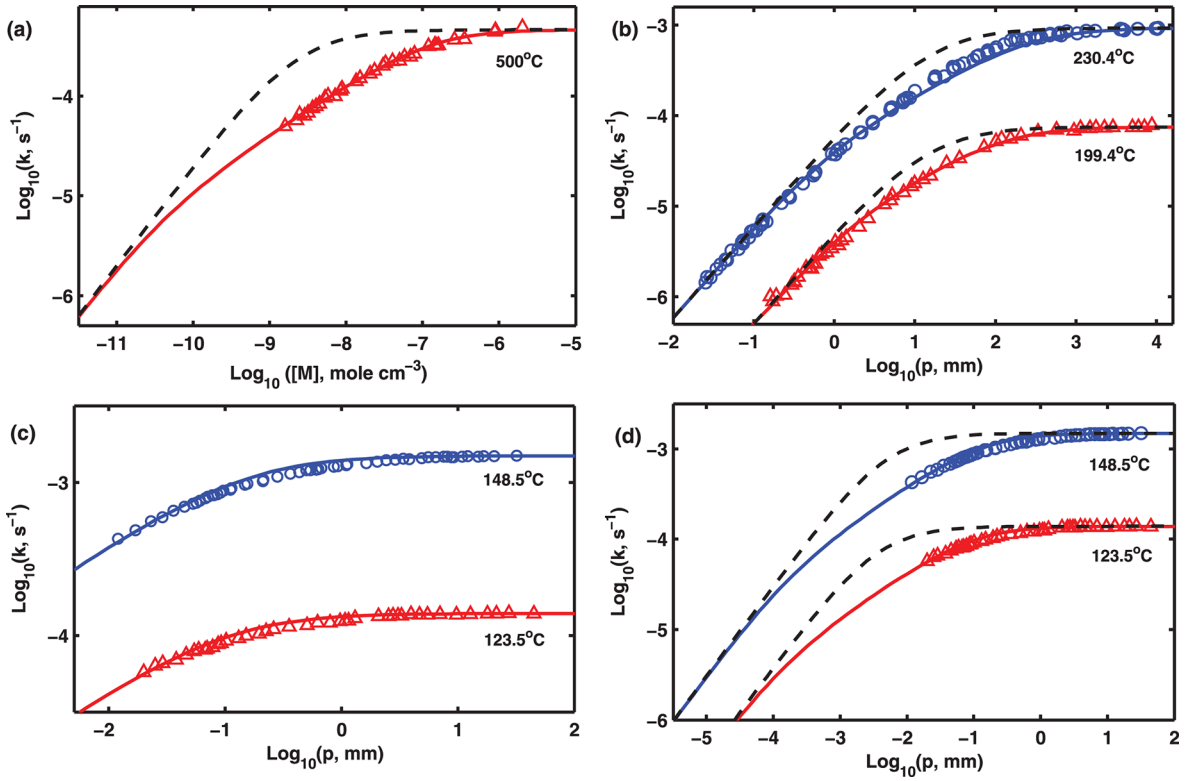

Figure 1. Falloff curves for (a) the isomerization of cyclopropane, (b) the isomerization of CH_3NC, and (c, d) the isomerization of 3-methylcyclobutene. Points are experimental data from refs 25, 26, and 27, respectively; solid lines are the effective rate constant, k^{slk} obtained from the SLK approach using the fitting parameters tabulated in Table 1. Dashed lines in parts a, b, and d are the classical effective rate constant, $k^{cl} = (k_2k_1[M])/(k_{-1}[M] + k_2)$ for the same fitting parameters. Parts a, b, and d show that k^{slk} coincides with k^{cl} in the limiting cases of very low and high $[M]$.

done, for instance, in recent work in enzyme kinetics.[32] This results in

$$k^{slk} = \frac{\langle\tau\rangle^{-1}}{N} = (N\int_0^\infty d\tau\tau w(\tau|N))^{-1} \quad (8)$$

where k^{slk} is the effective rate constant obtained from the SLK approach. The above equation suggests that under steady state conditions, the reciprocal of the mean waiting time for the formation of first product is related to the initial rate of the formation of product. Thus, the limits of infinitely large, $[M]_\infty$, and vanishingly small, $[M]_0$, concentrations correspond to the deterministic and single-molecule stochastic Lindemann kinetics respectively. In the former case, $k^{slk}_\infty = k^{cl}_\infty = k_1k_2/k_{-1}$, and in the latter case, $k^{slk}_0 = k^{cl}_0 = k_1[M]_0$. In between these two limiting cases, eq 6 suggests systematic deviations from the classical Lindemann equation, resulting in a nonlinear variation of $\langle\tau\rangle$ as a function of $[M]$.

To study this nonlinear variation, we compute the mean waiting time $\langle\tau\rangle$ exactly from the first moment of the waiting time distribution, eq 4, numerically. The reciprocal of the mean waiting time is related to the effective rate constant k^{slk}, eq 8, which is compared directly with the experimental data.[22−27]

COMPARISON WITH EXPERIMENTAL DATA

In the SLK method, the effective rate constant, k^{slk} [eq 8], which is obtained from the reciprocal of the first moment of the waiting time distribution [eq 4] by numerical quadrature, depends on $k^{slk}(k_1,k_{-1}/N,k_2/N,[M])$, where k_1, k_{-1}/N and k_2/N are three independent fitting parameters. Our analytical analysis show that $k^{slk}(k_1,k_{-1}/N,k_2/N,[M])$ approaches k^{cl}[eq 1] at very high and low $[M]$ given by $k^{cl}_\infty = k_1k_2/k_{-1}$ at $[M]_\infty$ and $k^{cl}_0/[M]_0 = k_1$ at $[M]_0$, respectively. The values of these three fitting parameters are obtained by fitting k^{slk} [eq 8] to available experimental data at a given temperature, which let us suppose yields $k_1 = k_1^*$, $k_{-1}/N = k_{-1}^*$, and $k_2/N = k_2^*$. Once the values of these three fitting parameters are known, the effective rate constant $k^{slk}(k_1 = k_1^*,k_{-1}/N = k_{-1}^*,k_2/N = k_2^*,[M])$ can be evaluated at any value of $[M]$ using eqs 4 and 8. To obtain k^{slk}_∞, $k^{slk}(k_1^*,k_{-1}^*,k_2,[M])$ is extrapolated to large $[M]$ limit,

$$k^{slk}(k_1^*, k_{-1}^*, k_2^*, [M])|_{[M]\to\infty} = k^{slk}_\infty(k_1^*, k_{-1}^*, k_2^*, [M]_\infty) \equiv k^{cl}_\infty = k_1^*k_2^*/k_{-1}^* \quad (9)$$

such that at and beyond $[M]_\infty$, k^{slk} approaches a constant value, which is close to the classical result, $k^{cl}_\infty = k_1^*k_2^*/k_{-1}^*$.

Similarly, to obtain k^{slk}_0, $k^{slk}(k_1^*,k_{-1}^*,k_2^*,[M])$ is extrapolated to small $[M]$ limit,

$$\left.\frac{k^{slk}(k_1^*, k_{-1}^*, k_2^*, [M])}{[M]}\right|_{[M]\to 0} = \frac{k^{slk}_0(k_1^*, k_{-1}^*, k_2^*, [M]_0)}{[M]_0} \equiv k^{cl}_0/[M]_0 = k_1^* \quad (10)$$

such that at and below $[M]_0$, $k^{slk}/[M]$ approaches a constant value, which is close to the classical result, $k^{cl}_0/[M]_0 = k_1^*$.

Thus, the fitting parameters in the SLK method not only fit $k^{slk}(k_1,k_{-1}/N,k_2/N,[M])$ to available experimental data, but the extrapolated values also yield $k^{cl}_0/[M]_0 = k_1$ and $k^{cl}_\infty = k_1k_2/k_{-1}$ at $[M]_0$ and $[M]_\infty$ given by $k^{slk}_0(k_1,k_{-1}/N,k_2/N,[M]_0)/[M]_0 = k_1$ and $k^{slk}_\infty(k_1,k_{-1}/N,k_2/N,[M]_\infty) = k_1k_2/k_{-1}$, respectively. Since $k^{cl}_\infty = k_1k_2/k_{-1}$ and $k^{cl}_0/[M]_0 = k_1$ depend on the combination of the three independent fitting parameters, the above two equations

dx.doi.org/10.1021/jp402675s | J. Phys. Chem. A 2013, 117, 7661−7669

Table 1. Fitting Parameters (k_1, k_{-1}/N and k_2/N) for the Reaction Types: (1) Isomerization of Cyclopropane, (2) Isomerization of CH_3NC, (3) Isomerization of 3-Methylcyclobutene at Various Temperatures[a]

Reaction Types	T (°C)	$*p^{expt}/^{\dagger}[M]^{expt}$ range	k_1 ($cm^3\ mol^{-1}\ s^{-1}$)	k_{-1}/N ($cm^3\ mol^{-1}\ s^{-1}$)	$k_2/N \times 10^4$ (s^{-1})	k_{∞}^{expt} (s^{-1})	k_{∞}^{slk} ($*p_{\infty}/^{\dagger}[M]_{\infty}$) ($s^{-1}$)
1	500.0	$^{\dagger}(10^{-9}-10^{-6})$	2.0×10^5	6.90×10^3	0.16	4.9×10^{-4}	4.6×10^{-4} ($^{\dagger}10^{-4}$)
2	199.4	$*(10^{-1}-10^{4})$	1.50×10^2	0.385×10^2	0.193	7.5×10^{-5}	7.5×10^{-5} ($*10^5$)
	230.4	$*(10^{-2}-10^{4})$	1.85×10^3	2.0×10^2	1.0	9.25×10^{-4}	9.23×10^{-4} ($*10^5$)
3	123.5	$*(10^{-2}-10^{2})$	9.50×10^5	6.82×10^4	0.10	1.39×10^{-4}	1.39×10^{-4} ($*10^2$)
	148.5	$*(10^{-2}-10^{2})$	8.0×10^6	5.36×10^5	1.0	1.49×10^{-3}	1.49×10^{-3} ($*10^2$)

[a]Units of p and $[M]$ are mm and mol/cm^3, respectively. For the values of fitting parameters tabulated below, k^{slk} is obtained from eq 8 and extrapolated to high $p_{\infty}/[M]_{\infty}$ such that k_{∞}^{slk} attains a constant value. The latter is close to $k_{\infty}^{cl} = k_1k_2/k_{-1}$.

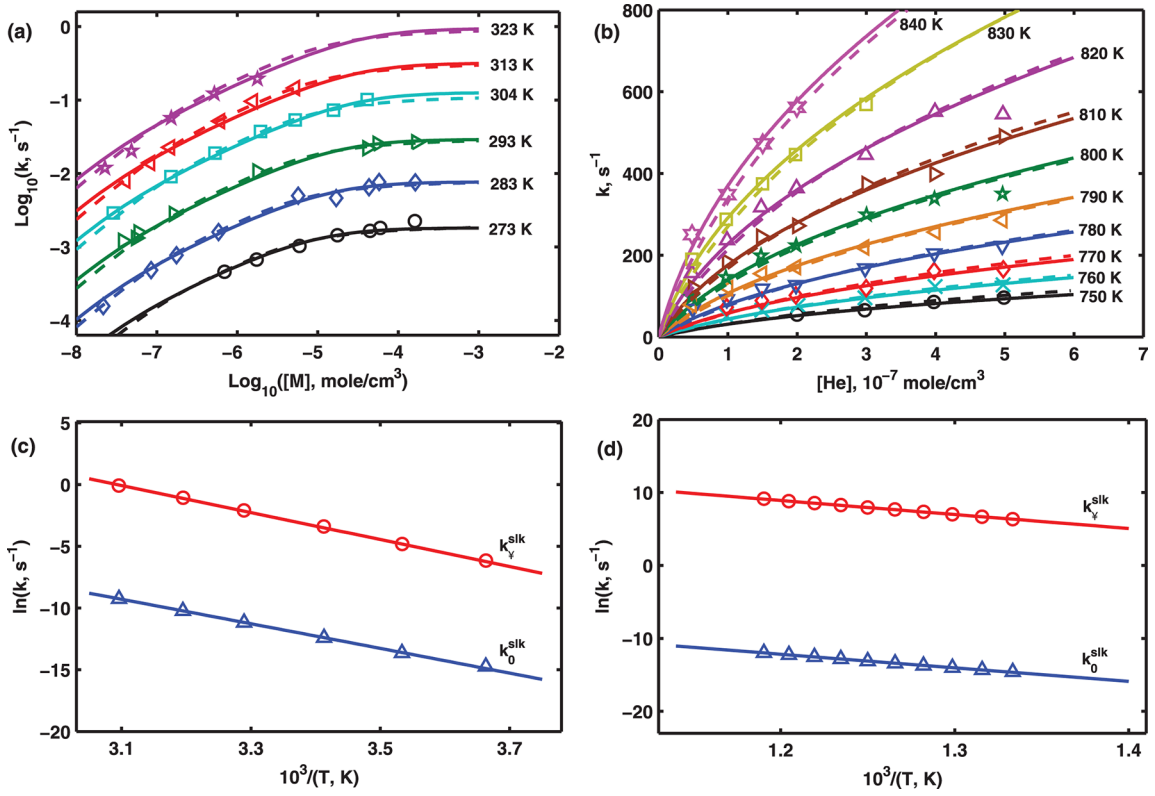

Figure 2. Falloff curves for (a) the decomposition of N_2O_5 (in N_2 bath gas) and (b) the decomposition of iso-C_3H_7 (in He bath gas). Points are experimental data from refs 22 and 23, respectively, at different temperatures; solid lines are the effective rate constant, k^{slk} obtained from the SLK approach using the fitting parameters tabulated in Tables 2 and 3, respectively. Dashed lines are the effective rate constant obtained from the Troe semi empirical (TSE) [eq 11] method using the fitting parameters specified by eqs 12 and 13. Modified Arrhenius plots (c) for the decomposition of N_2O_5 and (d) for the decomposition of iso-C_3H_7. Points are the extrapolated values of k^{slk} in low, k_0^{slk}, and high, k_{∞}^{slk}, concentration limits of inert gas molecules at different temperatures, tabulated in Tables 2 and 3, respectively. The solid lines are fit to the modified Arrhenius expressions given by eqs 14 and 15, respectively.

are self-consistent equations. The SLK method, therefore, provides a self-consistent way to check the consistency of the extrapolated results. It is to be noted that while k_0^{slk}, k_0^{cl}, and k_{∞}^{slk} are extrapolated values, k_{∞}^{cl} is a derived result.

In what follows, considering k_1, k_{-1}/N, and k_2/N as the temperature dependent empirical parameters, $k^{slk}(k_1,k_{-1}/N,k_2/N,[M])$ is fitted to the experimentally available data points, k^{expt} for the decomposition of N_2O_5,[22] iso-C_3H_7,[23] isobutane,[24] *n*-butane,[24] isomerization of cyclopropane,[25] methyl isocyanide,[26] and 3-methyl cyclobutene,[27] at different temperatures.

Figure 1a–d shows the falloff curves for the isomerization of cyclopropane at 500 °C,[25] the isomerization of methyl isocyanide at 199.4 °C, 230.4 °C,[26] and the isomerization of 3-methyl cyclobutene at 123.5 °C, 148.5 °C,[27] respectively. Assuming all the gases as ideal, the variation of the effective rate constant with pressure is calculated by expressing $[M]$ in terms of p, that is, $[M] = p/RT$. The SLK approach [solid lines in Figure 1a–d] shows excellent fit to the experimental data in the entire concentration range of M in which experimental data are reported.

Moreover, Figure 1, parts a, b, and d, shows that the effective rate constant obtained from the classical Lindemann equation, k^{cl} [dotted lines] coincides with the SLK approach k^{slk} [solid lines] in the limit of very low and high concentrations of inert gas molecules yielding $k_0^{slk} = k_0^{cl} = k_1[M]_0$ and $k_{\infty}^{slk} = k_{\infty}^{cl} = k_1k_2/k_{-1}$, respectively. This is in agreement with the approximate analytical analysis presented in eqs 5–8.

The values of the fitting parameters used in plotting Figures 1a–d are tabulated in Table 1 along with the pressure/concentration range $[p^{expt}/[M]^{expt}]$ in which the fittings of k^{slk} with k^{expt} were obtained. Using these fitting parameters, k^{slk} can be extrapolated to low and high concentration range, until $k_0^{slk}/[M]_0$ and k_{∞}^{slk} attain constant values, to yield the low and high

dx.doi.org/10.1021/jp402675s | J. Phys. Chem. A 2013, 117, 7661–7669

Table 2. Fitting Parameters (k_1, k_{-1}/N and k_2/N) for Unimolecular Decomposition of N_2O_5 at Various Temperatures[a]

T (K)	$k_1 \times 10^{-5}$ (cm^3 mol^{-1} s^{-1})	$k_{-1}/N \times 10^{-4}$ (cm^3 mol^{-1} s^{-1})	$k_2/N \times 10^2$ (s^{-1})	$k_0^{slk} \times 10^5$ (s^{-1})	$k_\infty^{slk} \times 10^1$ (s^{-1})	$k_0^{cl} \times 10^5$ (s^{-1})	$k_\infty^{cl} \times 10^1$ (s^{-1})
273	0.034	0.04	0.022	0.04	0.021	0.034	0.019
283	0.12	0.115	0.074	0.12	0.079	0.12	0.077
293	0.41	0.35	0.25	0.41	0.334	0.41	0.293
304	1.40	0.99	0.90	1.40	1.23	1.40	1.27
313	3.60	2.40	2.13	3.60	3.37	3.60	3.20
323	9.55	5.90	5.85	9.53	9.30	9.55	9.47

[a]For the values of fitting parameters tabulated below, k^{slk} is obtained from eq 8 and extrapolated to very low $[M]_0 = 10^{-10}$ mol/cm^3 and high $[M]_\infty = 10^6$ mol/cm^3 such that $k_0^{slk}/[M]_0$, k_∞^{slk} and $k_0^{cl}/[M]_0 = k_1$ attain constant values. The value of $k_\infty^{cl} = k_1k_2/k_{-1}$ is derived from the fitting parameters.

Table 3. Fitting Parameters (k_1, k_{-1}/N and k_2/N) for Unimolecular Decomposition of iso-C_3H_7 at Various Temperatures[a]

T (K)	$k_1 \times 10^{-9}$ (cm^3 mol^{-1} s^{-1})	$k_{-1}/N \times 10^{-8}$ (cm^3 mol^{-1} s^{-1})	$k_2/N \times 10^{-2}$ (s^{-1})	$k_0^{slk} \times 10$ (s^{-1})	$k_\infty^{slk} \times 10^{-3}$ (s^{-1})	$k_0^{cl} \times 10$ (s^{-1})	$k_\infty^{cl} \times 10^{-3}$ (s^{-1})
750	0.42	0.93	1.29	0.42	0.58	0.42	0.58
760	0.59	1.29	1.79	0.59	0.82	0.59	0.82
770	0.81	1.50	2.09	0.81	1.13	0.81	1.13
780	1.11	1.98	2.77	1.11	1.55	1.11	1.55
790	1.51	2.50	3.52	1.51	2.12	1.51	2.13
800	2.04	2.90	4.10	2.04	2.88	2.04	2.88
810	2.73	3.00	4.26	2.73	3.87	2.73	3.88
820	3.64	3.57	5.09	3.64	5.18	3.64	5.19
830	4.81	4.19	6.00	4.81	6.88	4.81	6.89
840	6.33	4.87	7.00	6.32	9.09	6.33	9.10

[a]For the values of fitting parameters tabulated below, k^{slk} is obtained from eq 8 and extrapolated to very low $[M]_0 = 10^{-10}$ mol/cm^3 and high $[M]_\infty = 10^{-1}$ mol/cm^3 such that $k_0^{slk}/[M]_0$, k_∞^{slk}, and $k_0^{cl}/[M]_0 = k_1$ attain constant values. The value of $k_\infty^{cl} = k_1k_2/k_{-1}$ is derived from the fitting parameters.

concentration limits of the effective rate constants. The last column of Table 1 shows the values of $p_\infty/[M]_\infty$ at which the k^{slk} attain a constant values given by $k_\infty^{slk}(p_\infty/[M]_\infty)$, which are close to the classical values $k_\infty^{cl} = k_1k_2/k_{-1}$. These values are in excellent agreement with the experimental values, k_∞^{expt}.

Below, we compare the SLK approach with the most widely used Troe semiempirical method (TSE) of data analysis to show that the values of the empirical parameters obtained by fitting k^{slk} to k^{expt} provides accurate estimates for the effective rate constant even outside the fitting range in which experimental data are inaccessible.

Comparison of the Stochastic Lindemann Kinetics Approach with the Troe Semiempirical Method of Data Analysis. The TSE method of data analysis modifies the Lindemann–Hinshelwood model by introducing a correction term due to strong and weak collision broadening effects, F_c, which has a simple analytic expression, rendering the effective rate constant at low, k_0, and high, k_∞, concentrations of inert gas molecules, and F_c as the temperature dependent empirical parameters. Using k_0, k_∞, and F_c as the input parameters, the TSE method fits the experimentally inaccessible values of the effective rate constant at low and high concentrations of M to experimentally accessible concentrations. The underlying equation for the TSE method is given by

$$k^{tse}(T) = \left[\frac{k_0[M]}{1 + k_0[M]/k_\infty}\right] F_c^{(1+[(\log(k_0[M]/k_\infty)/N_1]^2)^{-1}} \quad (11)$$

where $N_1 = 0.75-1.27 \log F_c$. Using the above equation, the falloff curves can be constructed provided reliable estimates for k_0 and k_∞ can be found. Below, we present a case study of four well-studied reactions in the literature—the unimolecular decomposition of N_2O_5[22] and iso-C_3H_7[23] and the thermal decomposition of isobutane and n-butane[24] to compare the TSE approach with the SLK approach.

We first compare the experimental data for the decomposition of N_2O_5 and iso-C_3H_7, where accessible range cover 4 orders of magnitude [10^{-8}–10^{-4} mol/cm^3] and an order of magnitude [10^{-8}–10^{-7} mol/cm^3] in the concentration of inert gas molecules, respectively. The dotted and solid lines in Figure 2a and b are the respective TSE and SLK fits to the experimental data for the decomposition of N_2O_5 and iso-C_3H_7.

For the decomposition of N_2O_5, where the experimentally accessible concentration range is wide, the TSE method yields,[22]

$$\begin{aligned} k_0^{tse}(T)/[M]_0 &= 6.26 \times 10^{20}(T/300)^{-3.5} \\ &\quad e^{-11000/T}\ cm^3\ mol^{-1}\ s^{-1} \\ k_\infty^{tse}(T) &= 6.22 \times 10^{14}(T/300)^{-0.2}e^{-11000/T}\ s^{-1} \\ F_c(T) &= 2.5e^{-1950/T} + 0.9e^{-T/430} \end{aligned} \quad (12)$$

For the decomposition of iso-C_3H_7, however, the experimentally accessible concentration range is too narrow to yield reliable estimates for k_∞^{tse}. Thus, the TSE method [eq 11] in combination with the RRKM/ME approach yield,[23]

$$\begin{aligned} k_0^{tse}(T)/[M]_0 &= 6.05 \times 10^{15}(T)^{1.1}e^{-17793/T}\ cm^3\ mol^{-1}\ s^{-1} \\ k_\infty^{rrkm}(T) &= 6.51 \times 10^{7}(T)^{1.83}e^{-17793/T}\ s^{-1} \\ F_c(T) &= 4.3e^{-T/640} - 1.35e^{-450/T} \end{aligned} \quad (13)$$

where the superscripts tse and rrkm refer to the effective rate constants in the low and high concentration range obtained using the TSE and RRKM/ME methods, respectively. These parameters are fit to the modified Arrhenius expression, $k = A(T/T_0)^n e^{-E_0/T}$, where T_0 is the reference temperature and n is the temperature exponent.

The temperature dependent empirical parameters for the SLK approach, k_1,k_{-1}/N,k_2/N, obtained by fitting the experimentally

dx.doi.org/10.1021/jp402675s | J. Phys. Chem. A 2013, 117, 7661–7669

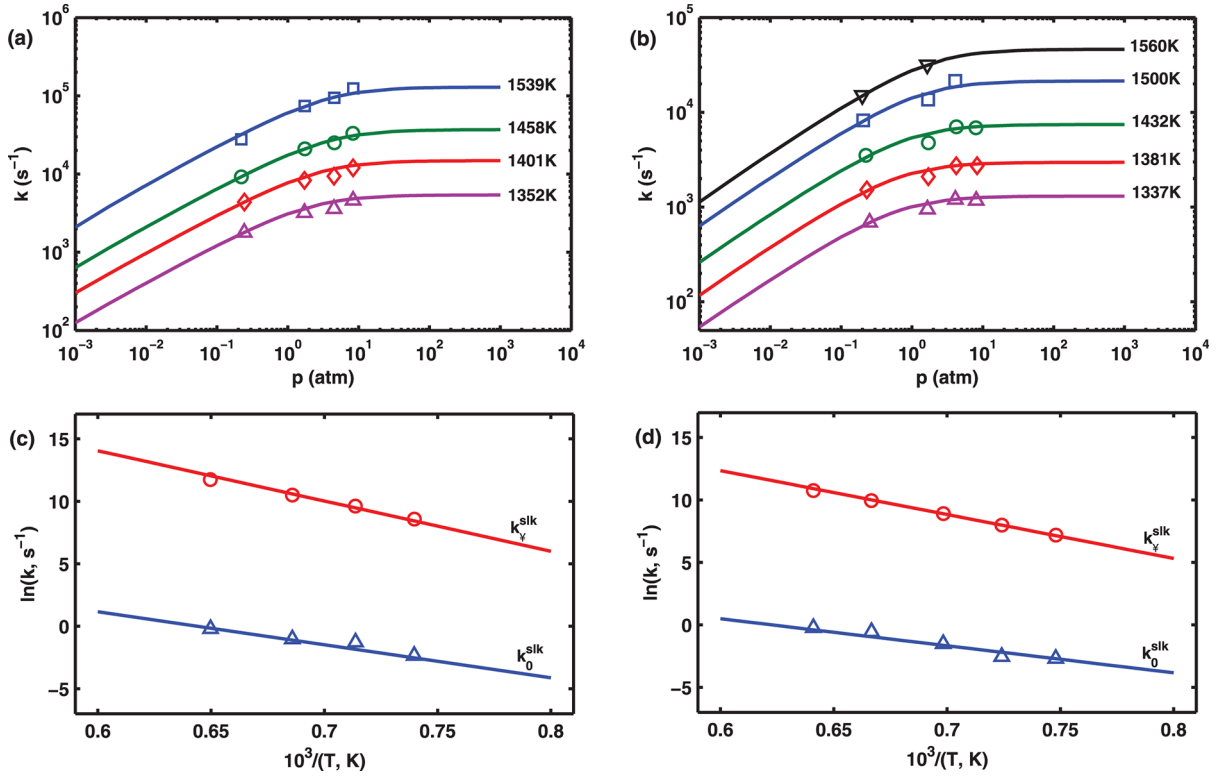

Figure 3. Falloff curves for the decomposition of (a) isobutane and (b) *n*-butane (in Argon bath gas). Points are experimental data from ref 24 at different temperatures; solid lines are the effective rate constant, k^{slk} obtained from the SLK approach using the fitting parameters tabulated in Table 4. Modified Arrhenius plots (c) for the decomposition of isobutane and (d) for the decomposition of *n*-butane. Points are the extrapolated values of k^{slk} in low, k_0^{slk}, and high, k_∞^{slk}, concentration limits of inert gas molecules at different temperatures, tabulated in Table 4. The solid lines are fit to the modified Arrhenius expressions given by eqs 18 and 19, respectively.

accessible data range for the decomposition of N_2O_5 and iso-C_3H_7 are tabulated in Tables 2 and 3, respectively. The extrapolated values of k^{slk} at low and high concentrations of $[M]$, yield k_0^{slk} and k_∞^{slk}, respectively. These values are reported in Table 2 and 3 along with the values of $[M]_0$ and $[M]_\infty$ at which these extrapolations were carried out. The extrapolated and derived values of k_0^{cl} and k_∞^{cl} are also given in Tables 2 and 3 for comparison.

To compare the extrapolated values of the SLK approach with the values obtained from the Troe semiempirical (TSE) method given by eqs 12 and 13, we plot the extrapolated values, $\ln(k_\infty^{slk})$ and $\ln(k_0^{slk})$, as a function of the reciprocal of temperature [Figures 2c and d]. The circles and triangles in Figures 2c and 2d correspond to the extrapolated values, k_∞^{slk} and k_0^{slk}, respectively, which are reported in Tables 2 and 3 along with the respective temperatures. The solid lines in Figure 2c and d are fits to the modified Arrhenius expressions, $k = A(T/300)^n e^{-E_0/T}$ and $k = A(T)^n e^{-E_0/T}$ corresponding to eq 12 and eq 13 respectively, where A, n, and E_0 are considered as the fitting parameters. To compare the temperature dependence of the extrapolated values in the SLK method with the values obtained in the TSE method, we keep the values of n and E_0 same as eqs 12 and 13, and vary A to fit the extrapolated values, represented as points in Figure 2c and d. The resulting modified Arrhenius expression fit for the decomposition of N_2O_5 represented as solid line in Figure 2c yields

$$k_0^{slk}(T)/[M]_0 = 7.65 \times 10^{20}(T/300)^{-3.5} e^{-11000/T} \text{ cm}^3 \text{ mol}^{-1} \text{ s}^{-1}$$
$$k_\infty^{slk}(T) = 6.03 \times 10^{14}(T/300)^{-0.2} e^{-11000/T} \text{ s}^{-1} \quad (14)$$

Similarly, the resulting modified Arrhenius expression fit for the decomposition of iso-C_3H_7 represented as solid line in Figure 2d yields

$$k_0^{slk}(T)/[M]_0 = 5.92 \times 10^{15}(T)^{1.1} e^{-17793/T} \text{ cm}^3 \text{ mol}^{-1} \text{ s}^{-1}$$
$$k_\infty^{slk}(T) = 6.22 \times 10^{7}(T)^{1.83} e^{-17793/T} \text{ s}^{-1} \quad (15)$$

This shows that the extrapolated values of $k_{0/\infty}^{slk}$ obtained from the SLK approach [eq 14] are in close agreement with values obtained from the TSE method, $k_{0/\infty}^{tse}$ [eq 12]. It can be verified that the extrapolated values in Tables 2 and 3 yield $k_\infty^{cl} = k^{cl} = k_1k_2/k_{-1}$ and $k_0^{slk}/[M]_0 = k_0^{cl}/[M]_0 = k_1$ given by 9 and 10, respectively.

In order to further test the accuracy of the values obtained from the extrapolation of k^{slk}, we consider the experimental data for the thermal decomposition of isobutane and *n*-butane,[24] available in a narrow pressure range of 0.1−10 atm. In this narrow range, the TSE method in conjunction with the RRKM/ME method,[24] for the decomposition of isobutane,

dx.doi.org/10.1021/jp402675s | J. Phys. Chem. A 2013, 117, 7661−7669

Table 4. Fitting Parameters (k_1, k_{-1}/N, and k_2/N) for the Reaction Types: (1) Thermal Decomposition of Isobutane and (2) Decomposition of *n*-Butane at Various Temperatures[a]

reaction types	T (K)	$k_1 \times 10^{-10}$ ($cm^3\ mol^{-1}\ s^{-1}$)	$k_{-1}/N \times 10^{-8}$ ($cm^3\ mol^{-1}\ s^{-1}$)	$k_2/N \times 10$ (s^{-1})	$k_0^{slk} \times 10^2$ (s^{-1})	$k_\infty^{slk} \times 10^{-4}$ (s^{-1})	$k_0^{cl} \times 10^2$ (s^{-1})	$k_\infty^{cl} \times 10^{-4}$ (s^{-1})
1	1352	9.6	5.6	3.2	9.6	0.53	9.6	0.55
	1401	28.0	12.0	6.5	28.0	1.46	28.0	1.52
	1458	36.0	24.0	25.0	36.0	3.64	36.0	3.75
	1539	82.0	88.0	140.0	82.0	1.27	82.0	1.31
2	1337	6.8	4.2	0.82	6.8	0.13	6.8	0.13
	1381	7.9	9.5	3.6	7.9	0.29	7.9	0.29
	1432	22.0	19.0	6.5	21.9	0.74	22.0	0.75
	1500	58.0	40.0	15.0	57.8	2.13	58.0	2.18
	1560	79.0	64.0	38.0	78.8	4.60	79.0	4.69

[a]For the values of fitting parameters tabulated below, k^{slk} is obtained from eq 8 and extrapolated to very low $[M]_0 = 10^{-12}$ mol/cm^3 ($p_0 = 10^{-7}$ atm) and high $[M]_\infty = 10^{-3}$ mol/cm^3 ($p_\infty = 10^2$ atm), such that $k_0^{slk}/[M]_0$, k_∞^{slk} and $k_0^{cl}/[M]_0 = k_1$ attain constant values. The value of $k_\infty^{cl} = k_1k_2/k_{-1}$ is derived from the fitting parameters.

$$k_{0,1}^{rrkm}(T)/[M]_0 = 2.41 \times 10^{19} e^{-26460K/T}\ cm^3\ mol^{-1}\ s^{-1}$$
$$k_{\infty,1}^{rrkm}(T) = 4.83 \times 10^{16} e^{-40210K/T}\ s^{-1}$$
$$F_{c,1}(T) = 0.98 e^{-T/750} \quad (16)$$

and *n*-butane yield

$$k_{0,2}^{rrkm}(T)/[M]_0 = 5.34 \times 10^{17} e^{-21620K/T}\ cm^3\ mol^{-1}\ s^{-1}$$
$$k_{\infty,2}^{rrkm}(T) = 4.28 \times 10^{14} e^{-35180K/T}\ s^{-1}$$
$$F_{c,2}(T) = 0.41 e^{-T/1500} \quad (17)$$

Figure 3a and b is the SLK fits to the experimental data for the thermal decomposition of isobutane and *n*-butane for the empirical rate constants tabulated in Table 4. Using these empirical rate constants, k^{slk} can be extrapolated to the low and high concentration range to yield k_0^{slk} and k_∞^{slk}. Figure 3c and d show the variation of $\ln(k_\infty^{slk})$ (circles) and $\ln(k_0^{slk})$ (triangles) as a function of the reciprocal of temperature [Table 4]. To compare the extrapolated values in the SLK method with the values obtained in the TSE method, we fit the Arrhenius expression $k = Ae^{-E_0/T}$ corresponding to eqs 16 and 17 to the extrapolated values, represented as points in Figure 3c and d. The Arrhenius expression fits for the decomposition of isobutane and *n*-butane are obtained by keeping E_0 same as that of eqs 16 and 17 and varying A. The solid lines in Figures 3c and 3d are fits to the following expressions:

$$k_{0,1}^{slk}(T)/[M]_0 = 2.5 \times 10^{19} e^{-26460K/T}\ cm^3\ mol^{-1}\ s^{-1}$$
$$k_{\infty,1}^{slk}(T) = 3.8 \times 10^{16} e^{-40210K/T}\ s^{-1} \quad (18)$$

$$k_{0,2}^{slk}(T)/[M]_0 = 7.0 \times 10^{17} e^{-21620K/T}\ cm^3\ mol^{-1}\ s^{-1}$$
$$k_{\infty,2}^{slk}(T) = 3.4 \times 10^{14} e^{-35180K/T} s^{-1} \quad (19)$$

Again, the extrapolation of k^{slk} outside the narrow fitting range yield $k_{0/\infty}^{slk}$ [eqs 18 and 19] in close agreement with the values obtained from the TSE method [eqs 16 and 17], respectively. Once again, it can be verified that the extrapolated values in Table 4 yield $k_\infty^{slk} = k_\infty^{cl} = k_1k_2/k_{-1}$ and $k_0^{slk}/[M]_0 = k_0^{cl}/[M]_0 = k_1$ given by 9 and 10, respectively. As has been explained earlier that in obtaining the temperature dependence of the extrapolated values [Figures 2c, d, 3c, d] given by eqs 14, 15, 18, and 19, a priori knowledge of the values of n and E_0 in eqs 12 and 13 and the values of E_0 in eqs 16 and 17 have been used.

CONCLUSIONS

We have reformulated, here, the classical Lindemann kinetics for unimolecular gas-phase reactions by considering each step of the Lindemann mechanism as intrinsically stochastic. Our stochastic Lindemann kinetics (SLK) is described by a chemical master equation (CME) for the joint probability of the number of reactants, intermediates, and products at any instant of time. An exact analytical solution of this CME has been obtained from which the probability distribution of the duration required for a product to be formed for the first time can be obtained. The effective rate constant of the gas phase reaction is related to the mean duration for the formation of the first product. This relation is utilized to provide a new semiempirical method for analyzing experimental data in unimolecular gas-phase kinetics. The effective rate constant, k^{slk} computed by the SLK method provides excellent agreement with experimental data[22−27] in the entire concentration range of inert gas molecules in which data is available. The SLK method provides a self-consistent extrapolation formula from which the rate constants at experimentally inaccessible ranges of concentrations can be obtained from the experimentally accessible measured values. A detailed analysis of four well-studied gas phase reactions in N_2O_5, iso-C_3H_7, and isobutane/*n*-butane has been presented to validate the SLK method. Stochastic Lindemann kinetics, thus, provides a simple, self-consistent method for the analysis of kinetic data in the entire range of concentrations of the inert gas molecules and can be used as an alternative to the widely used Troe semiempirical (TSE) method of data analysis for unimolecular gas-phase reaction kinetics.

APPENDIX: EXACT SOLUTION OF THE WAITING TIME DISTRIBUTION FROM THE CME

In CME [eq 2] the constraint $n_a + n_{a^*} + n_p = N$ can be introduced by marginalizing with respect to one of the variables,

$$P(n_{a^*}, n_p, t|N) = \sum_{n_a} \delta_{n_a+n_{a^*}+n_p,N} P(n_a, n_{a^*}, n_p, t)$$

The marginalized CME is given by

dx.doi.org/10.1021/jp402675s | J. Phys. Chem. A 2013, 117, 7661−7669

$$\frac{\partial P(n_{a*}, n_p, t|N)}{\partial t} = k_m(N - n_{a*} - n_p + 1)P(n_{a*} - 1, n_p, t|N) + k_{-m}(n_{a*} + 1)P(n_{a*} + 1, n_p, t|N) + k_2(n_{a*} + 1)P(n_{a*} + 1, n_p - 1, t|N) - [k_m(N - n_{a*} - n_p) + (k_{-m} + k_2)n_{a*}]P(n_{a*}, n_p, t|N) \quad (A1)$$

The solution of the marginalized CME can be obtained by using the generating function[28,29] defined as

$$G(s_1, t|N) = \sum_{n_{a*}=0} s_1^{n_{a*}} P(n_{a*}, 0, t|N) \quad (A2)$$

Thus, the equation of motion for the generating function is given by

$$\frac{\partial G(s_1, t|N)}{\partial t} = -k_m N(1 - s_1)G(s_1, t|N) + [(1 - s_1)(k_n + k_m s_1) - k_2]\frac{\partial G(s_1, t|N)}{\partial s_1} \quad (A3)$$

where $k_n = k_{-m} + k_2$. The above equation for the generating function can be solved by the method of characteristics, which yields

$$G(s_1, t|N) = \left[\frac{k_2 - (1 - s_1)(k_n + k_m s_1)}{k_2 \beta^r}\right]^{N/2} \Omega[\beta \exp(-k_2' t)] \quad (A4)$$

where Ω is an unknown function, the form of which can be determined in such a way that the initial conditions are satisfied. Also,

$$r = \frac{k_m + k_n}{k_2'}, \quad \beta = \frac{k_2' + (k_m + k_n)}{k_2' - (k_m + k_n)}\left(\frac{k_2' - k_2'}{k_2' + k_2'}\right) \quad (A5)$$

$$k_2' = k_n + (2s_1 - 1)k_m, \quad k_2' = \sqrt{(k_m + k_n)^2 - 4k_m k_2} \quad (A6)$$

Using the initial condition, $P(n_{a*},0,0|N) = \delta_{na*,0}$, in eq A2 yields

$$G(s_1, 0|N) = 1 = \left[\frac{k_2 - (1 - s_1)(k_n + k_m s_1)}{k_2 \beta^r}\right]^{N/2} \Omega[\beta] \quad (A7)$$

resulting in

$$\Omega[\beta] = \left[\frac{k_2 - (1 - s_1)(k_n + k_m s_1)}{k_2 \beta^r}\right]^{-N/2} \quad (A8)$$

Replacing β with a temporary variable X in eqs A5 and A6 yields the following expression for s_1 in terms of X:

$$s_1 = \frac{1}{2}\left[\frac{k_2'}{k_m}\left\{\frac{(1 - X) + r(1 + X)}{(1 + X) - r(1 - X)}\right\} - \frac{k_n}{k_m} + 1\right] \quad (A9)$$

which, after much simplification, yields

$$\Omega[X] = \frac{1}{2^N}[X^{r-1/2}\{(1 + X) + r(1 - X)\}]^N \quad (A10)$$

Introducing $X = \beta \exp(-k_2' t)$ and inserting eq A10 into eq A4, the expression for the generating function is given by

$$G(s_1, t|N) = \frac{1}{2^N}\left[\frac{k_2' + k_2'}{k_2'}\exp[-((k_m + k_n) - k_2')t/2] + \frac{k_2' - k_2'}{k_2'}\exp[-((k_m + k_n) + k_2')t/2]\right]^N \quad (A11)$$

which, after simplification, yields the following expression for the generating function:

$$G(s_1, t|N) = \frac{1}{2^N}\left[e^{-(\lambda_2 - \lambda_1)t} + e^{-(\lambda_2 + \lambda_1)t} + \frac{k_2'}{2\lambda_1}(e^{-(\lambda_2 - \lambda_1)t} - e^{-(\lambda_2 + \lambda_1)t})\right]^N \quad (A12)$$

where $\lambda_1 = ((k_m + k_n)^2 - 4k_m k_2/2)^{1/2}$ and $\lambda_2 = (k_m + k_n)/2$.

Differentiating eq A2 with respect to t and taking $s_1 = 1$ and $t = \tau$,

$$\frac{\partial G(1, t|N)}{\partial t}|_{t=\tau} = \sum_{n_{a*}} \frac{\partial P(n_{a*}, 0, t|N)}{\partial t}|_{t=\tau} \quad (A13)$$

From eq A3,

$$\frac{\partial G(1, t|N)}{\partial t}|_{t=\tau} = -k_2 \frac{\partial G(s_1, \tau|N)}{\partial s_1}|_{s_1=1} \quad (A14)$$

Combining eqs A13 and A14

$$\sum_{n_{a*}} \frac{\partial P(n_{a*}, 0, t|N)}{\partial t}|_{t=\tau} = -k_2 \frac{\partial G(s_1, \tau|N)}{\partial s_1}|_{s_1=1} \quad (A15)$$

Equation A15 when substituted into eq 3 yields the following expression for the waiting time distribution:

$$w(\tau|N) = k_2 \frac{\partial G(s_1, \tau|N)}{\partial s_1}|_{s_1=1} \quad (A16)$$

From eq A12,

$$\frac{\partial G(s_1, \tau|N)}{\partial s_1}|_{s_1=1} = \frac{N k_m}{2^N \lambda_1}[e^{-(\lambda_2 - \lambda_1)\tau} - e^{-(\lambda_2 + \lambda_1)\tau}] \times \left[e^{-(\lambda_2 - \lambda_1)\tau} + e^{-(\lambda_2 + \lambda_1)\tau} + \frac{k_n + k_m}{2\lambda_1}(e^{-(\lambda_2 - \lambda_1)\tau} - e^{-(\lambda_2 + \lambda_1)\tau})\right]^{N-1} \quad (A17)$$

Equation A17 when substituted into eq A16 yields eq 4.

AUTHOR INFORMATION

Corresponding Author

*E-mail: arti@iitm.ac.in.

Notes

The authors declare no competing financial interest.

ACKNOWLEDGMENTS

S.S. acknowledges the financial support from the University Grants Commision (UGC), Government of India.

REFERENCES

(1) Lindemann, F. A. Discussion on the Radiation Theory of Chemical Action. *Trans. Faraday Soc.* **1922**, *17*, 598−606.
(2) Rice, O. K.; Ramsperger, H. C. Theories of Unimolecular Gas Reactions at Low Pressures. *J. Am. Chem. Soc.* **1927**, *49*, 1616−1629.
(3) Kassel, L. S. Studies in Homogeneous Gas Reactions I. *J. Phys. Chem.* **1928**, *32*, 225−242.
(4) Wieder, G. M.; Marcus, R. A. Dissociation and Isomerization of Vibrationally Excited Species. II. Unimolecular Reaction Rate Theory and Its Application. *J. Chem. Phys.* **1962**, *37*, 1835−1852.
(5) Marcus, R. A. Dissociation and Isomerization of Vibrationally Excited Species. III. *J. Chem. Phys.* **1965**, *43*, 2658−2661.
(6) Gilbert, R. G.; Smith, S. C. *Theory of Unimolecular and Recombination Reactions*; Blackwell Scientific Publications: Oxford, 1990.
(7) Holbrook, K. A.; Pilling, M. J.; Robertson, S. H. *Unimolecular Reactions*, 2nd ed.; John Wiley & Sons: New York, 1996.
(8) Forst, W. *Theory of Unimolecular Reactions*; Academic Press: New York, 1973.
(9) Troe, J. Fall-off Curves of Unimolecular Reactions. *Ber. Bunsenges. Phys. Chem.* **1974**, *78*, 478−488.
(10) Troe, J. *Physical Chemistry: An Advanced Treatise. Vol. VIB, Kinetics of Gas Reactions*; Academic: New York, 1975; pp 835−929.
(11) Troe, J. Predictive Possibilities of Unimolecular Rate Theory. *J. Phys. Chem.* **1979**, *83*, 114−126.
(12) Troe, J. Theory of Thermal Unimolecular Reactions in the Fall-off Range. I. Strong Collision Rate Constants. *Ber. Bunsenges. Phys. Chem.* **1983**, *87*, 161−169.
(13) Gilbert, R. G.; Luther, K.; Troe, J. Theory of Thermal Unimolecular Reactions in the Fall-off Range. II. Weak Collision Rate Constants. *Ber. Bunsenges. Phys. Chem.* **1983**, *87*, 169−177.
(14) Kaiser, E. W.; Wallington, T. J. Kinetics of the Reactions of Chlorine Atoms with C_2H_4 (k_1) and C_2H_2 (k_2): A Determination of $\Delta H_{f,298}$ for C_2H_3. *J. Phys. Chem.* **1996**, *100*, 4111−4119.
(15) Lovejoy, E. R.; Hanson, D. R. Kinetics and Products of the Reaction $SO_3 + NH_3 + N_2$. *J. Phys. Chem.* **1996**, *100*, 4459−4465.
(16) Forster, R.; Frost, M.; Fulle, D.; Hamann, H. F.; Hippler, H. High Pressure Range of the Addition of HO to HO, NO, NO_2, and CO. I. Saturated Laser Induced Fluorescence Measurements at 298 K. *J. Chem. Phys.* **1995**, *103*, 2949−2958.
(17) Fulle, D.; Hamann, H. F.; Hippler, H.; Troe, J. High Pressure Range of the Addition of HO to HO. III. Saturated Laser Induced Fluorescence Measurements between 200 and 700 K. *J. Chem. Phys.* **1996**, *105*, 1001−1006.
(18) Fulle, D.; Hamann, H. F.; Hippler, H. The Pressure and Temperature Dependence of the Recombination Reaction $HO^{\bullet} + SO_2 + M \rightarrow HOSO_2^{\bullet} + M$. *Phys. Chem. Chem. Phys.* **1999**, *1*, 2695−2702.
(19) Yang, X.; Jasper, A. W.; Kiefer, J. H.; Tranter, R. S. The Dissociation of Diacetyl: A Shock Tube and Theoretical Study. *J. Phys. Chem. A* **2009**, *113*, 8318−8326.
(20) Baasandorj, M.; Knight, G.; Papadimitriou, V. C.; Talukdar, R. K.; Ravishankara, A. R.; Burkholder, J. B. Rate Coefficients for the Gas-Phase Reaction of the Hydroxyl Radical with CH_2 = CHF and CH_2 = CF_2. *J. Phys. Chem. A* **2010**, *114*, 4619−4633.
(21) Altinay, G.; Macdonald, R. G. Determination of the Rate Constants for the $NH_2(X^2B1)$ + $NH_2(X^2B1)$ and $NH_2(X^2B1)$ + H Recombination Reactions with Collision Partners CH_4, C_2H_6, CO_2, CF_4, and SF_6 at Low Pressures and 296 K. Part 2. *J. Phys. Chem. A* **2012**, *116*, 2161−2176.
(22) Cantrell, C. A.; Shetter, R. E.; Calvert, J. G.; Tyndall, G. S.; Orlando, J. J. Measurement of Rate Coefficients for the Unimolecular Decomposition of N_2O_5. *J. Phys. Chem.* **1993**, *97*, 9141−9148.
(23) Seakins, P. W.; Robertson, S. H.; Pilling, M. J.; Slagle, I. R.; Gmurczyk, G. W.; Bencsura, A.; Gutman, D.; Tsang, W. Kinetics of the Unimolecular Decomposition of iso-C_3H_7: Weak Collision Effects in Helium, Argon, and Nitrogen. *J. Phys. Chem.* **1993**, *97*, 4450−4458.
(24) Oehlschlaeger, M. A.; Davidson, D. F.; Hanson, R. K. High-Temperature Thermal Decomposition of Isobutane and *n*-Butane behind Shock Waves. *J. Phys. Chem. A* **2004**, *108*, 4247−4253.
(25) Johnston, H. S.; White, J. R. Statistical Interpretations of Unimolecular Reaction Rates. *J. Chem. Phys.* **1954**, *22*, 1969−1973.
(26) Schneider, F. W.; Rabinovitch, B. S. The Thermal Unimolecular Isomerization of Methyl Isocyanide. Fall-off Behavior. *J. Am. Chem. Soc.* **1962**, *84*, 4215−4230.
(27) Frey, H. M.; Marshall, D. C. Thermal Unimolecular Isomerization of Cyclobutenes. Part 5. The Isomerization of 3-Methylcyclobutene at Low Pressures. *Trans. Faraday Soc.* **1965**, *61*, 1715−1721.
(28) Gardiner, C. W. *Handbook of Stochastic Methods for Physics, Chemistry and the Natural Sciences*, 3rd ed.; Springer: New York, 2004.
(29) Van Kampen, N. G. *Stochastic Processes in Physics and Chemistry*, 3rd ed.; Elsevier: New York, 2007.
(30) Saha, S.; Ghose, S.; Adhikari, R.; Dua, A. Nonrenewal Statistics in the Catalytic Activity of Enzyme Molecules at Mesoscopic Concentrations. *Phys. Rev. Lett.* **2011**, *107*, 218301.
(31) Daley, D. J.; Vere-Jones, D. *An Introduction to the Theory of Point Processes*, 2nd ed.; Springer: New York, 2003; Vol. *1*.
(32) English, B. P.; Min, W.; van Oijen, A. M.; Lee, K. T.; Luo, G.; Sun, H.; Cherayil, B. J.; Kou, S. C.; Xie, X. S. Ever-Fluctuating Single Enzyme Molecules: Michaelis−Menten Equation Revisited. *Nat. Chem. Biol.* **2006**, *2*, 87−94.